the cross section for the excitation of this level with the (d,p) reaction will be relatively low.[5]

Other levels in ^{35}S predicted by Glaudemans, all with positive parity, cannot correspond to the levels found at 1.99 and 2.35 MeV, as the latter have negative parity[1]; moreover these levels were seen by Endt in the (d,p) reaction on ^{34}S, whereas the levels calculated by Glaudemans will not be excited in a stripping reaction.[5] Further, Watson *et al.*[7] have investigated resonance states in ^{35}Cl with the (p,γ) reaction on ^{34}S and they have found two negative-parity states in ^{35}Cl at the correct energies to be the isobaric analogs of the 1.99- and 2.35-MeV states in ^{35}S.

The 1.99-MeV level in ^{35}S would then correspond to the 7.54-MeV state in ^{35}Cl, which is a $\frac{7}{2}^-$ state. If we tentatively assign a J^π value of $\frac{1}{2}^+$ to the 1.56-MeV level in ^{35}S, the decay of the 1.99-MeV level to only the $\frac{3}{2}^+$ ground state confirms a $\frac{7}{2}$ spin for this level; a cascade through the 1.56-MeV level would imply an octupole transition. Erné[8] has made shell-model calculations on odd-parity levels in nuclei in the range ^{33}S–^{41}Ca and he finds a $\frac{7}{2}^-$ level in ^{35}S at an excitation energy of 2.32 MeV, which might correspond to the 1.99-MeV level in that nucleus.

If the experimentally determined 2.35-MeV state in ^{35}S is the isobaric analog state of the 7.84-MeV level in ^{35}Cl, an assignment of $\frac{3}{2}^-$ is not in disagreement with the decay scheme of this state, again assuming a J^π of $\frac{1}{2}^+$ for the 1.56-MeV level.

ACKNOWLEDGMENT

We wish to thank Dr. Ph. B. Smith and the other members of the Van de Graaff group for their advice and assistance.

[7] D. D. Watson, J. C. Manthuruthil, and F. D. Lee, Phys. Rev. **164**, 1399 (1967).

[8] F. C. Erné, Nucl. Phys. **84**, 91 (1966).

PHYSICAL REVIEW VOLUME 173, NUMBER 4 20 SEPTEMBER 1968

Inelastic Electron Scattering from ^{26}Mg at 180°

W. L. Bendel, L. W. Fagg, R. A. Tobin, and H. F. Kaiser
Nuclear Physics Division, U. S. Naval Research Laboratory, Washington, D. C. 20390
(Received 3 April 1968)

The 180° inelastic electron scattering from ^{26}Mg has been studied at bombarding energies of 39 and 56 MeV. Eight magnetic dipole transitions are found from 1+ states at 8.52, 9.24, 9.67, 10.18, 10.63, 11.20, 13.33, and 13.66 MeV. The transition radii and ground-state radiation widths are calculated.

I. INTRODUCTION

THE study of nuclear structure by means of electron scattering is done in practice either (1) at 180° or (2) at a range of other angles. The experimenter who chooses 180° scattering must employ more complex apparatus than that required for other angles and cannot readily adapt his apparatus to other angles of scattering. In addition, one must expect small scattering cross sections at 180°.

On the other hand, the data at 180° serves as a valuable complement to that from other angles because it has a unique advantage. Effectively, only the transverse component of the cross section is nonzero. Usually this means that magnetic transitions, which are often overshadowed at other angles, are the most prominent features at 180°. This is demonstrated rather effectively in the work reported here on ^{26}Mg, where many magnetic dipole transitions are found. We discuss the properties of these transitions and also, briefly, the relationship of the results to the theoretical work of Morpurgo[1] and Kurath.[2]

II. THEORETICAL FRAMEWORK

The data are analyzed using the model-independent theoretical expressions given by Rosen *et al.*[3] This results in the determination of the multipolarity of the transition, the transition radius, and the strength (B or Γ_0) of the transition.

As our electron scattering data are taken at 180°, we assume a magnetic transition of multipolarity 2^L and obtain [Ref. 3, Eq. (5)]

$$\left(\frac{d\sigma}{d\Omega}\right)_{180^\circ} = \frac{\pi\alpha}{[(2L+1)!!]^2}\frac{L+1}{L}\frac{q^{2L}}{k_1^2}B(ML,q), \quad (1)$$

where k_1 is the initial electron momentum; q, the momentum transfer; and B, the reduced transition proba-

[1] G. Morpurgo, Phys. Rev. **110**, 721 (1958).
[2] D. Kurath, Phys. Rev. **130**, 1525 (1963).
[3] M. Rosen, R. Raphael, and H. Überall, Phys. Rev. **163**, 927 (1967).

bility. The q dependence of B is given by [Ref. 3, Eq. (13a)]

$$\left[\frac{B(ML,q)}{B(ML,0)}\right]^{1/2}=1-\frac{L+3}{L+1}\frac{(qR)^2}{2(2L+3)}+\frac{L+5}{L+1}\frac{(qR^*)^4}{8(2L+3)(2L+5)}, \quad (2)$$

where R and R^* are transition radii as defined in Ref. 3.

Combining Eqs. (1) and (2) for given L, one obtains $d\sigma/d\Omega$ as a function of measurable momenta plus $B(ML,O)$, R, and R^*. In principle, one could solve for these three quantities with cross-section measurements taken at three or more energies. In practice, electron scattering measurements are much too inaccurate to determine R^* from the small fourth-order term. Theoretically one expects $R\approx R^*$, so it is both permissible and convenient to set $R=R^*$ here. One may now solve for two parameters with cross sections measured at two energies. If the correct value of L has been chosen, R should approximately equal the nuclear matter radius.

The ground-state radiation width is given by [Ref. 3, Eq. (15a)]

$$\Gamma_0=\frac{8\pi}{[(2L+1)!!]^2}\frac{L+1}{L}\frac{2J_0+1}{2J+1}\omega^{2L+1}B(ML,\omega), \quad (3)$$

where ω is the excitation energy, and J_0 and J are the ground- and excited-state spins, respectively.

A somewhat more detailed discussion of the theoretical considerations as well as of the data treatment is given in another paper.[4]

III. APPARATUS

Linac and Beam Handling System

Electrons are accelerated in the USNRL 60-MeV linear accelerator, a three-section S-band machine,[5] using 360 pulses per sec. When operating at 56 MeV, all sections are used; at 39 MeV, only two linac sections are usually powered.

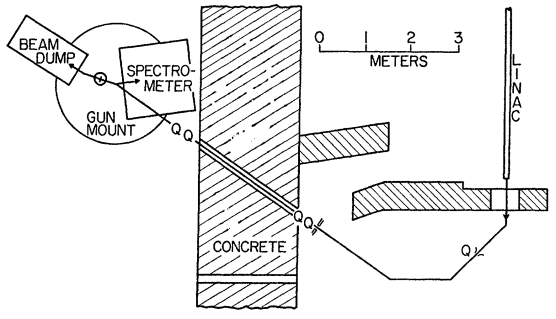

FIG. 1. Path of the electron beam employed for electron scattering. Deflection magnets are at the points where the beam bends. Quadrupole magnets are indicated by Q.

As indicated in Fig. 1, the beam employed for electron scattering is energy analyzed by an achromatic magnetic system[6] consisting of two flat-field 45°-deflection magnets and a quadrupole magnet singlet midway between them. The first deflection magnet[7] analyzes the beam into a momentum spectrum at the position of the quadrupole. The momentum-defining slit is placed here. In the work reported in this paper, this slit is set to transmit a beam of 0.4% full width. A beam of 2 μA has been typical under these conditions, although 5 μA now has become common at 56 MeV.

The beam for this experiment is switched by a 35° magnet[7] toward the scattering apparatus. En route, it passes a nonmagnetic steel aperture of 9-mm diameter and 13-mm thickness, a quadrupole doublet, diagonally through a 2.13-m concrete wall (2.60 m along the beam path) into the experiment room, another quadrupole doublet, and then into the electron scattering apparatus. In addition, the system includes steering coils and three movable scintillating beam probes.

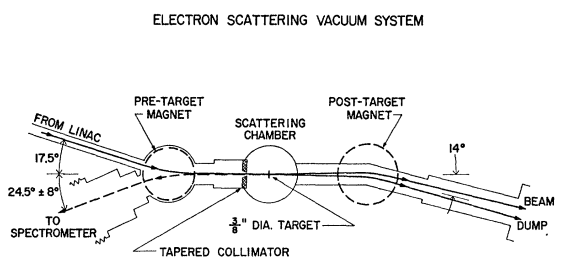

FIG. 2. The electron scattering vacuum system, viewed from above.

Electron Scattering Apparatus

As seen in Fig. 2, the electron beam from the linac is deflected 17.5° by the pre-target magnet into the scattering chamber. It is about 3 mm in diameter as it strikes the thin target in the center of the scattering chamber. From the target, almost all of the electrons in the beam continue forward in a narrow cone, are deflected 14° by another magnetic field, and are stopped in a beam dump.

The beam dump consists of an aluminum vacuum chamber inside a lead shield. In the direct path of the beam is 9.8 cm of graphite followed by aluminum and lead. The beam dump is electrically isolated by a glass section in the vacuum pipe. The current is integrated by a voltage-to-frequency converter and a scaler which turns off the electron counting equipment when the selected charge has been accumulated.

[4] L. W. Fagg, W. L. Bendel, R. A. Tobin, and H. F. Kaiser, Phys. Rev. **171**, 1250 (1968).

[5] T. F. Godlove, R. A. Tobin, and J. McElhinney, Navy Technical Forum, 1963 (unpublished); also Rept. NRL Progr. (U.S.), Jan. 1964, p. 1 (unpublished).

[6] S. Penner, Rev. Sci. Instr. **32**, 150 (1961).

[7] T. F. Godlove and W. L. Bendel, Rev. Sci. Instr. **36**, 909 (1965).

Electrons scattered 180° by the target re-enter the magnetic field of the pre-target magnet and are deflected into the spectrometer vacuum system. Electrons scattered at small forward angles by the target will hit the vacuum chamber and the beam pipes, and some will then be back-scattered, as will some electrons from the beam dump. The post-target magnet and a permanent magnet at the entrance of the beam dump are employed to reduce the number of backstreaming electrons. In addition, a tapered copper and nonmagnetic steel aperture, 2.38 cm thick and 1.27 cm in diameter, is placed in front of the target. This aperture is adequate to accept the desired cone of scattered electrons from the target, but it greatly reduces the number of undesired electrons going to the detection system.

Any of several targets, including a scintillator, may be moved into the target position. The target is viewed by a closed-circuit television system, using glass ports on the scattering chamber. By this means, target and beam may be positioned.

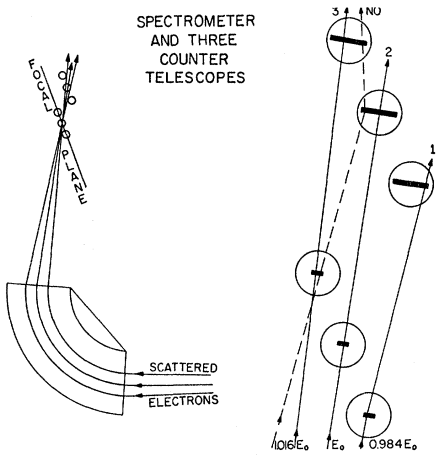

FIG. 3. The spectrometer bends 180°-scattered electrons of energy E_0 upward 100° and focuses them on the center counter telescope, as shown on the left. Three counting channels are employed, as shown in the expanded view on the right. The dashed line shows the path of an electron which is not counted because of the anticoincidence requirement.

Analysis

The spectrometer and detectors are mounted on a "5-in." naval gun mount. The center of the pre-target magnet is on the axis of this gun mount. The beam piping includes a flexible bellows so that the spectrometer may be positioned anywhere within the range 24.5°±8°, as shown in Fig. 2. The angle to be employed is calculated from the momentum of the electrons to be detected.

The double-focusing magnetic spectrometer, of 25-cm orbit radius, deflects electrons of the proper momentum 100° upward, as shown on the left in Fig. 3. As the 180°-scattered electrons go through the field of the pre-target magnet as well as the spectrometer magnet, the focusing properties of the two magnets must be considered together. The field of the spectrometer is proportional to the momentum of the detected electrons after scattering. On the other hand, the field of the pre-target magnet is set for the momentum of the incident electrons and the gun mount is rotated to the angle of deflection of the scattered electrons to be detected.

By tracing rays, using a computer, it is found that the radial (i.e., momentum-dependent) focal plane of the system is almost independent of the relative magnetic fields and, therefore, fixed detectors may be employed. In the axial direction of the spectrometer, the focal plane does change with relative field. Fortunately, this is of little importance since sufficiently long scintillators are employed. The solid-angle acceptance of the system is also dependent upon the relative fields.

Detection

As shown on the right in Fig. 3, three channels, each consisting of a detector telescope and associated equipment, count the electrons. The first detector is a Pilot B scintillator, 1.59×4.76×25.4 mm, in the radial focal plane of the magnetic system and on an Amperex XP1115 photomultiplier tube. The second detector of each pair is larger, 1.59×15.88×33.9 mm. The smaller detectors are each 0.50% wide and they are 1.55% apart, in electron momentum.

Pulses from the detectors are fed, via discriminators, into three coincidence analyzers of 10 nsec full resolving time. Each coincidence analyzer receives pulses from three detectors—the two detectors of a given channel and the one other detector most likely to scatter electrons into the second detector of that channel. A coincidence count requires pulses from both detectors of the given channel and no pulse from the other detector. A trigger pulse from the linac gates the counting system on for 3 μsec with each linac beam pulse.

Energy Calibration

The initial energy calibrations of the magnets in the system were based on the field measurements and ray tracings required in the design and construction of the apparatus. When the electron scattering work reached a satisfactory stage, a new energy calibration—in satisfactory agreement with the original computed calibrations—was adopted, using the level in ^{12}C at 15.110 MeV. At nominal incident energies of 39 and 56 MeV, the elastic peak and the 15.1-MeV peak from a 55.8-mg/cm^2 graphite target are observed. The constant relating magnetic field, as measured by a rotating-coil probe, to electron momentum is then calculated from these peaks. In the case of the spectrometer, the uncertainty in the calibration is 0.11%.

IV. RESULTS

The target is a disk of magnesium, enriched to 99.78% ^{26}Mg, 9.5 mm in diameter and 72.7 mg/cm^2 in thickness.

In a normal set of runs, the spectrometer field is changed in steps corresponding to a fraction (usually $\frac{1}{8}$) of the space between detectors. The same point on the spectrum is thus "counted" in turn, by each counter channel, and the counts added. The total number of coincidences is plotted against either electron momentum or nuclear excitation energy.

Except for the elastic peak, needed as the "zero" of excitation, most of the ^{26}Mg data were collected for excitations of 8 to 15 MeV. The results obtained with 2000 μC of electrons with an incident kinetic energy of 55.8 MeV are shown in Fig. 4. The results from 1000 μC at 38.8 MeV are shown in Fig. 5. Eight corresponding peaks are seen in the two sets of data; the level energies shown are the averages obtained from the results at both bombardment energies. Three other small peaks are shown on one or the other figure. The "net counts" are those remaining after no-target background has been subtracted and the counts then normalized to a standard solid angle and channel width (in MeV).

In order to determine cross sections, the areas under the peaks were integrated and then corrected with the Schwinger,[8] bremsstrahlung,[8] and ionization[9] corrections. The results are given in Table I. As relative cross sections are used in some calculations, the uncertainties shown on the cross sections represent only the statistical uncertainties in the data. In addition to these counting statistics, we estimate a 15% uncertainty in the absolute cross sections, primarily due to uncertainties in the above three corrections and in counter efficiency. As these uncertainties largely cancel out in determining the transition radius R from the ratio of cross sections, the uncertainty given for R is that due to counting statistics. The values tabulated for the partial-radiation width Γ_0 include the 15% uncertainty from other sources.

The last column of Table I shows the transitions found in the electron scattering work of Titze and Spamer[10] at energies similar to ours, but not at 180°. They have labeled these transitions as M (magnetic) and/or E (electric), without specifying multipolarity, based on the angular dependence and q dependence of their results. Their paper does not include cross sections, radiation widths, or transition radii for ^{26}Mg levels.

V. DISCUSSION

The five best-measured levels are at 9.24, 10.18, 10.63, 11.20, and 13.33 MeV. Each is readily identified with a single level which Titze and Spamer[10] have labeled as M or $M+E$. Their average energy is 0.01 MeV greater than our average, though most individual differences are greater.

When treated as magnetic-dipole transitions, these five cases yield a weighted-average transition radius of 3.39 fm, which is equal to $1.14A^{1/3}$ fm. This value is a reasonable radius for ^{26}Mg. We conclude that these are $M1$ transitions from the 0+ ground state to 1+ excited states.

The calculated transition radii of the three other levels which appear in both sets of data also indicate $M1$ transitions, although the identifications are less certain. The lower limits of the transition radii as $M2$ transitions are $R=4.9$ fm for the level at 8.52 MeV, $R=5.3$ fm at 9.67 MeV, and $R=4.6$ fm at 13.66 MeV, all quite large for ^{26}Mg. The level at 9.67 MeV may well be the unresolved sum of the 9.58- and 9.80-MeV levels of Ref. 10 and thus treatment as a single level is open to question. The weak transition at 13.66 MeV appears as a shoulder on the largest peak, that at 13.33 MeV. This shoulder also appears in the 153° data of Ref. 10.

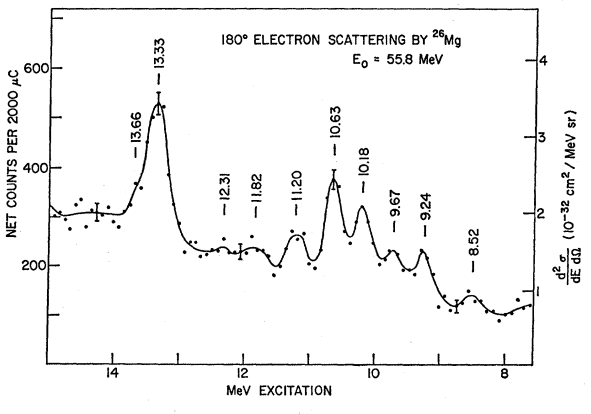

FIG. 4. Spectrum of electrons scattered at 180° by ^{26}Mg, using 55.8-MeV incident kinetic energy.

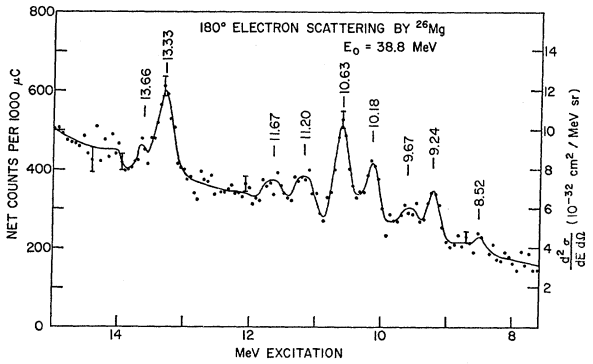

FIG. 5. Spectrum of electrons scattered at 180° by ^{26}Mg, using 38.8-MeV incident kinetic energy.

[8] D. B. Isabelle and G. R. Bishop, Nucl. Phys. **45**, 209 (1963).
[9] H. Breuer, Nucl. Instr. Methods **33**, 226 (1965).
[10] O. Titze and E. Spamer, Z. Naturforsch. **21a**, 1504 (1966).

TABLE I. Levels at 8 to 14 MeV in ^{26}Mg found in electron scattering. The differential cross sections are in units of 10^{-35} cm^2 per sr.

Energy (MeV)	$(d\sigma/d\Omega)_{56\ \mathrm{MeV}}$	$(d\sigma/d\Omega)_{39\ \mathrm{MeV}}$	Parameters as $M1$ transitions R (fm)	Γ_0 (eV)	Energy and type, Titze and Spamer[a]
					8.22 M
8.52±0.05	81±22	159±57	$3.2_{-1.4}{}^{+0.6}$	$0.5_{-0.3}{}^{+0.4}$	8.57 M
					8.91 E
9.24±0.03	268±26	695±63	$3.62_{-0.19}{}^{+0.17}$	$3.3_{-0.7}{}^{+0.9}$	9.25 M
9.67±0.05	246±26	409±69	$2.90_{-0.54}{}^{+0.36}$	$1.7_{-0.6}{}^{+0.8}$	9.58, 9.80 M
10.18±0.03	447±30	968±77	$3.40_{-0.18}{}^{+0.16}$	$5.7_{-1.2}{}^{+1.3}$	10.20 $M+(E)$
10.63±0.03	593±42	1332±77	3.47±0.14	$9.1_{-1.7}{}^{+2.0}$	10.67 $M+E$
11.20±0.05	274±26	525±68	$3.23_{-0.33}{}^{+0.26}$	$3.9_{-1.1}{}^{+1.3}$	11.17 $M+E$
11.67, 11.82					11.76 $E+M$
12.31	62±26	<97	<3.8	<1.2	12.26 M
					12.79 E
13.33±0.03	689±35	1174±90	$3.10_{-0.21}{}^{+0.17}$	$14.5_{-3.0}{}^{+3.3}$	13.34 M
13.66±0.06	110±31	180±76	$3.0_{-3.0}{}^{+0.8}$	$2.3_{-1.5}{}^{+2.4}$	

[a] See Ref. 10.

Kuehne *et al.*[11] have scattered photons from natural Mg. They find a level at 10.07±0.05 MeV that they identify with the ^{26}Mg electron scattering level at 10.2 MeV. They report $\Gamma_0^2/\Gamma=4.2$ eV, a value in agreement with our value of Γ_0 if the fractional decay to the ground state, Γ_0/Γ, is at least 0.5. The reported level energies, however, differ by slightly more than the sum of the uncertainties.

It is informative to compare our intensities with those shown in Fig. 2 of Titze and Spamer.[10] Employing Eqs. (1) and (2), we use the $M1$ transition radii to interpolate our cross sections to the q and k_1 of Ref. 10. (The interpolated value would be the same, within a few percent, for any other reasonable multipole assumed.) We may then correct to 153°, using the complete equations of Rosen *et al.*,[3] a correction which is the same for all magnetic multipoles and very nearly the same for all levels. Therefore, if all these transitions are magnetic, we would expect these cross sections to be proportional to those obtained from the corresponding peaks in Fig. 2 of Ref. 10. For the five best-measured levels, the ratios of observed to calculated 153° intensities (normalized so that their average is unity) are all in the range 0.90 to 1.09, in somewhat better agreement than the measurements warrant. The ratios for the three other levels are less accurately determined, particularly at 9.67 MeV, but are in satisfactory agreement.

One may also test the hypothesis that some of these transitions are electric multipoles. The transition radii were calculated assuming $E2$ transitions. These are essentially radii for the transverse component. They are larger than found for $M1$ transitions,[4,10,12] but approximately equal to transition radii found for the longitudinal component of $E2$ transitions.[10,12,13] Thus, we do not feel justified in ruling out $E2$ transitions on this basis. The comparison of 153° and 180° data, together with the theoretical equations,[3] however, consititutes a convincing test. Calculations were made of the ratios of cross sections at 153° to those at 178.3° (our effective angle) for $E1$, $E2$, and $E3$ transitions, employing the equations of Sec. II of Ref. 3. Using 3.40 fm for all transition radii involved, the ratio is almost independent of multipolarity, and ranges from 2.8 (at 13.66 MeV) to 6.8 (at 8.54 MeV) times the universal ratio for magnetic transitions. These ratios increase with assumed transition radius. Therefore it is clear that if any of the transitions considered here are magnetic, they all are. We conclude that eight magnetic-dipole transitions have been found.

The level at 12.31 MeV, seen only at 56-MeV bombardment, is weak relative to the 12.26-MeV level seen[10] at 153°, and may well be an electric transition, contrary to the assignment by Titze and Spamer.[10] The same is true of the level at 8.22 MeV, not seen here. Titze and Spamer[10] show a large peak at 11.76 MeV. We find only small peaks in this region and thus conclude that their result is largely due to an electric transition. They also report weak electric transitions at 8.91 and 12.79 MeV. We should not expect to, and do not, observe them.

It is interesting to note that prominent $M1$ transitions are more plentiful in ^{26}Mg than in ^{24}Mg in this energy range.[4] This is partially due to the Morpurgo[1] selection rule forbidding strong $M1$ transitions between levels with the same isospin T in self-conjugate nuclei. In addition, the $M1$ transition strength is concentrated in the lowest few $T=1$, 1+ levels in $4N$ nuclei (N is an integer) with $T=0$ ground state, as discussed by Kurath.[2] These predictions seem to be borne out by the work reported here and in Ref. 4.

ACKNOWLEDGMENTS

E. C. Jones, Miss Susan Numrich, and Dr. T. F. Godlove have each contributed in several roles to this work. We acknowledge many useful discussions with Professor H. Überall and Dr. M. Rosen. We wish to thank the linac operating staff for their cooperation in operating the accelerator.

[11] H. W. Kuehne, P. Axel, and D. C. Sutton, Phys. Rev. **163**, 1278 (1967).
[12] E. Spamer, Z. Physik **191**, 24 (1966).
[13] M. A. Duguay, C. K. Bockelman, T. H. Curtis, and R. A. Eisenstein, Phys. Rev. **163**, 1259 (1967).